# The NIR-SWIR combined atmospheric correction approach for MODIS ocean color data processing

**Menghua Wang* and Wei Shi**

*NOAA National Environmental Satellite, Data, and Information Service, Center for Satellite Applications and Research, E/RA3, Room 102, 5200 Auth Road, Camp Springs, MD 20746, USA*
**Corresponding author: Menghua.Wang@noaa.gov*

**Abstract:** A method of ocean color data processing using the combined near-infrared (NIR) and shortwave infrared (SWIR) bands for atmospheric correction for the Moderate Resolution Imaging Spectroradiometer (MODIS) on Aqua is proposed. MODIS-Aqua has been producing the high quality ocean color products in the open oceans, but there are still some significant errors in the derived products in the coastal regions. With the proposed NIR-SWIR combined algorithm, MODIS ocean color data can be processed using the standard (NIR) atmospheric correction algorithm for the open oceans, whereas for the turbid waters in the coastal region the SWIR atmospheric correction algorithm can be executed. The turbid water index developed by Shi and Wang (2007) (Remote Sens. Environ. **110**, 149-161 (2007)) is computed prior to the atmospheric correction for the identification of the productive and/or turbid waters where the SWIR algorithm can be operated. For non-turbid ocean waters (discriminated using the turbid water index criterion), the MODIS data are still processed using the standard (NIR) algorithm. The NIR-SWIR combined algorithm has been tested and evaluated. Two examples from MODIS-Aqua measurements along the U.S. and China east coast regions show improved ocean color products with the new approach. In particular, there are no obvious data discontinuities between using the NIR and SWIR methods. Therefore, with the NIR-SWIR combined approach for the MODIS ocean color data processing, good quality ocean color products can be derived both in clear (open) oceans as well as for turbid coastal waters.



**OCIS codes:** (010.0010) Atmosphere and ocean optics; (010.1285) atmospheric correction; (010.4450) ocean optics; (010.1290) atmospheric optics.

## References and links

1. C. R. McClain, G. C. Feldman, and S. B. Hooker, "An overview of the SeaWiFS project and strategies for producing a climate research quality global ocean bio-optical time series," Deep-Sea Research Part II-Topical Studies in Oceanography **51**, 5-42 (2004).
2. W. E. Esaias, M. R. Abbott, I. Barton, O. B. Brown, J. W. Campbell, K. L. Carder, D. K. Clark, R. L. Evans, F. E. Hodge, H. R. Gordon, W. P. Balch, R. Letelier, and P. J. Minnet, "An overview of MODIS capabilities for ocean science observations," IEEE Trans. Geosci. Remote Sens. **36**, 1250-1265 (1998).
3. H. R. Gordon, and M. Wang, "Retrieval of water-leaving radiance and aerosol optical thickness over the oceans with SeaWiFS: A preliminary algorithm," Appl. Opt. **33**, 443-452 (1994).
4. H. R. Gordon, "Atmospheric correction of ocean color imagery in the Earth Observing System era," J. Geophys. Res. **102**, 17,081-017,106 (1997).
5. S. W. Bailey, and P. J. Werdell, "A multi-sensor approach for the on-orbit validation of ocean color satellite data products," Remote Sens. Environ. **102**, 12-23 (2006).
6. M. Wang, K. D. Knobelspiesse, and C. R. McClain, "Study of the Sea-Viewing Wide Field-of-View Sensor (SeaWiFS) aerosol optical property data over ocean in combination with the ocean color products," J. Geophys. Res. **110**, D10S06, doi:10.1029/2004JD004950 (2005).

#87508 - $15.00 USD Received 14 Sep 2007; revised 6 Nov 2007; accepted 6 Nov 2007; published 12 Nov 2007

7. S. J. Lavender, M. H. Pinkerton, G. F. Moore, J. Aiken, and D. Blondeau-Patissier, "Modification to the atmospheric correction of SeaWiFS ocean color images over turbid waters," Continental Shelf Research **25**, 539-555 (2005).
8. K. G. Ruddick, F. Ovidio, and M. Rijkeboer, "Atmospheric correction of SeaWiFS imagery for turbid coastal and inland waters," Appl. Opt. **39**, 897-912 (2000).
9. D. A. Siegel, M. Wang, S. Maritorena, and W. Robinson, "Atmospheric correction of satellite ocean color imagery: the black pixel assumption," Appl. Opt. **39**, 3582-3591 (2000).
10. M. Wang, and W. Shi, "Estimation of ocean contribution at the MODIS near-infrared wavelengths along the east coast of the U.S.: Two case studies," Geophy. Res. Lett. **32**, L13606, doi:13610.11029/12005GL022917 (2005).
11. R. P. Stumpf, R. A. Arnone, R. W. Gould, P. M. Martinolich, and V. Ransibrahmanakul, "A partially coupled ocean-atmosphere model for retrieval of water-leaving radiance from SeaWiFS in coastal waters," NASA Tech. Memo. 2003-206892, S. B. Hooker and E. R. Firestone, eds. (NASA Goddard Space Flight Center, Greenbelt, Maryland, 2003), Vol. 22, pp. 51-59.
12. M. Wang, "Remote sensing of the ocean contributions from ultraviolet to near-infrared using the shortwave infrared bands: simulations," Appl. Opt. **46**, 1535-1547 (2007).
13. M. Wang, J. Tang, and W. Shi, "MODIS-derived ocean color products along the China east coastal region," Geophy. Res. Lett. **34**, L06611, doi:06610.01029/02006GL028599 (2007).
14. K. D. Knobelspiesse, C. Pietras, G. S. Fargion, M. Wang, R. Frouin, M. A. Miller, A. Subramaniam, and W. M. Balch, "Maritime aerosol optical properties measured by handheld sun photometers," Remote Sens. Environ. **93**, 87-106 (2004).
15. A. Smirnov, B. N. Holben, Y. J. Kaufman, O. Dubovik, T. F. Eck, I. Slutsker, C. Pietras, and R. N. Halthore, "Optical properties of atmospheric aerosol in maritime environments," J. Atmos. Sci. **59**, 501-523 (2002).
16. W. Shi, and M. Wang, "Detection of turbid waters and absorbing aerosols for the MODIS ocean color data processing," Remote Sens. Environ. **110**, 149-161 (2007).
17. M. Wang, and H. R. Gordon, "A simple, moderately accurate, atmospheric correction algorithm for SeaWiFS," Remote Sens. Environ. **50**, 231-239 (1994).
18. H. R. Gordon, and M. Wang, "Surface roughness considerations for atmospheric correction of ocean color sensors. 1: The Rayleigh scattering component," Appl. Opt. **31**, 4247-4260 (1992).
19. M. Wang, "The Rayleigh lookup tables for the SeaWiFS data processing: Accounting for the effects of ocean surface roughness," Int. J. Remote Sens. **23**, 2693-2702 (2002).
20. G. M. Hale, and M. R. Querry, "Optical constants of water in the 200nm to 200μm wavelength region," Appl. Opt. **12**, 555-563 (1973).
21. P. Y. Deschamps, M. Herman, and D. Tanre, "Modeling of the atmospheric effects and its application to the remote sensing of ocean color," Appl. Opt. **22**, 3751-3758 (1983).
22. M. Wang, "A sensitivity study of SeaWiFS atmospheric correction algorithm: Effects of spectral band variations," Remote Sens. Environ. **67**, 348-359 (1999).
23. M. Wang, "Aerosol polarization effects on atmospheric correction and aerosol retrievals in ocean color remote sensing," Appl. Opt. **45**, 8951-8963 (2006).
24. J. E. O'Reilly, S. Maritorena, B. G. Mitchell, D. A. Siegel, K. L. Carder, S. A. Garver, M. Kahru, and C. R. McClain, "Ocean color chlorophyll algorithms for SeaWiFS," J. Geophys. Res. **103**, 24,937-24,953 (1998).
25. H. R. Gordon, "Normalized water-leaving radiance: revisiting the influence of surface roughness," Applied Optics **44**, 241-248 (2005).
26. A. Morel, and G. Gentili, "Diffuse reflectance of oceanic waters: its dependence on Sun angle as influenced by the molecular scattering contribution," Appl. Opt. **30**, 4427-4438 (1991).
27. M. Wang, "Effects of ocean surface reflectance variation with solar elevation on normalized water-leaving radiance," Appl. Opt. **45**, 4122-4128 (2006).
28. S. Chen, G. Zhang, and S. Yang, "Temporal and spatial changes of suspended sediment concentration and resuspension in the Yangtze River estuary," J. Geographical Sciences **13**, 498-506 (2003).

## 1. Introduction

The ocean color satellite sensors Sea-viewing Wide Field-of-view Sensor (SeaWiFS) [1] and the Moderate Resolution Imaging Spectroradiometer (MODIS) [2] have provided us a view of chlorophyll patterns and ocean biospheres on global scales by using the advanced atmospheric correction algorithm for data processing [3,4]. For the global open oceans, both SeaWiFS and MODIS-Aqua have been producing high quality ocean color products [1,5,6], and these data have been used by researchers and scientists worldwide to study and understand ocean physical, optical, and biological changes and their effects on climatic processes. For the open ocean, the atmospheric correction for the SeaWiFS and MODIS has been carried out using the two near-infrared (NIR) bands with assumption of the negligible ocean contributions (black

#87508 - $15.00 USD Received 14 Sep 2007; revised 6 Nov 2007; accepted 6 Nov 2007; published 12 Nov 2007

ocean) at the two NIR bands [3,4]. However, in coastal regions, the current standard (NIR) data processing technique frequently produces considerable errors in the derived products due often to very turbid ocean waters for which the ocean has significant radiance contributions at the NIR bands [7-11]. The current SeaWiFS/MODIS algorithm has implemented a method to account for the NIR ocean contributions, based on a model of the spectral shape for particle backscattering coefficient in coastal waters [11]. Over the turbid ocean waters, however, there are still significant errors in the satellite-derived ocean color products due to model limitations for the complex turbid waters. In a recent development, an atmospheric correction algorithm using the shortwave infrared (SWIR) bands has been proposed [10,12] and demonstrated using the MODIS-Aqua measurements in the China east coastal region where waters are consistently extremely turbid [13]. Unfortunately, SeaWiFS does not have the SWIR bands. Although the SWIR method shows improved ocean color products in the coastal regions, its performance in the non-turbid ocean waters is usually worse than the standard (NIR) method with significant noise in the derived products. This is due mainly to the fact that the MODIS SWIR bands are designed for the land and atmosphere applications with substantially lower sensor band signal-noise ratio (SNR) values. For accurate ocean color products, much better sensor SNR values for the SWIR bands are required [12]. In addition, atmospheric correction using the SWIR bands often produces larger uncertainties than results from using the NIR bands, in particular, for cases of the maritime aerosols [12]. Open oceans are usually dominated with the maritime aerosols [6,14,15]. Therefore, for accurate MODIS ocean color data processing at each pixel level, the products for non-turbid waters should be produced using the standard (NIR) atmospheric correction algorithm, while for turbid coastal waters ocean color products should be derived using the SWIR approach.

In this paper, we describe and demonstrate a NIR-SWIR combined method for the atmospheric correction for the MODIS ocean color data processing. Following the recent work of *Shi and Wang* (2007) [16], pixels in ocean regions with significant ocean NIR contributions (i.e., turbid waters) can first be discriminated using MODIS measurements at the NIR and SWIR bands. The turbid water detection is operated prior to the atmospheric correction procedure and is very efficient [16]. For the identified turbid water pixels, the SWIR atmospheric correction algorithm can then be applied. For the most other pixels (non-turbid ocean waters), the standard (NIR) atmospheric correction algorithm can be employed. Thus, while the ocean color products in the coastal regions can be improved using the SWIR method, the MODIS high quality ocean color data in open oceans can be continuously produced. We describe the NIR-SWIR combined approach and provide results and discussions for testing and evaluation of the algorithm performance in coastal and open ocean regions with examples from MODIS-Aqua measurements along the U.S. and China east coastal regions.

## 2. The NIR-SWIR Combined Algorithm

### *2.1. Turbid Water Index*

Ocean waters in coastal regions are typically very productive, and often turbid. As such, in these regions the ocean could have a significant reflectance contribution at the NIR wavelengths (non-black) [7-11]. Recently, *Shi and Wang* (2007) [16] developed a method for the detection of the turbid waters using the turbid water index that are computed from the MODIS-measured radiances at the NIR and SWIR bands. The turbid water index, $T_{ind}(\lambda_i,\lambda_j)$, can be derived as [16,17]:

$$T_{ind}\left(\lambda_i,\lambda_j\right)=\frac{\Delta\rho^{(RC)}\left(\lambda_i\right)}{\Delta\rho^{(RC)}\left(\lambda_j\right)}\exp\left\{-\frac{\lambda_j-\lambda_i}{\lambda_k-\lambda_j}\ln\left(\frac{\Delta\rho^{(RC)}\left(\lambda_j\right)}{\Delta\rho^{(RC)}\left(\lambda_k\right)}\right)\right\}, \quad (1)$$

where $\Delta\rho^{(RC)}\left(\lambda_l\right)$ is the Rayleigh-corrected (RC) top-of-atmosphere (TOA) reflectance at a given wavelength [16], i.e.,

#87508 - $15.00 USD Received 14 Sep 2007; revised 6 Nov 2007; accepted 6 Nov 2007; published 12 Nov 2007

$$\Delta\rho^{(RC)}(\lambda_l) = \rho_t(\lambda_l) - \rho_r(\lambda_l) \tag{2}$$

and $\rho_t(\lambda_l)$ and $\rho_r(\lambda_l)$ are the sensor-measured TOA reflectance (with gas absorptions corrected) and the reflectance contributed from the molecules (Rayleigh scattering) [18,19], respectively. Using the MODIS-measured reflectances at the wavelengths $\lambda_i$ = 748 nm, $\lambda_j$ = 1240 nm, and $\lambda_k$ = 2130 nm, the turbid water index $T_{ind}$(748,1240) from Eq. (1) is defined as

$$T_{ind}(748,1240) = \frac{\Delta\rho^{(RC)}(748)}{\Delta\rho^{(RC)}(1240)} \exp\left\{-\frac{492}{890}\ln\left(\frac{\Delta\rho^{(RC)}(1240)}{\Delta\rho^{(RC)}(2130)}\right)\right\}. \tag{3}$$

Detection of the turbid waters using the parameter $T_{ind}$(748,1240) is based on the fact that for the productive ocean waters the ocean has a non-zero contribution at the NIR band 748 nm [16], while the black ocean is usually still true for the SWIR bands [10,20]. In Eq. (3), the ratio of reflectance at 748 and 1240 nm provides the turbid water detection, while the exponential term normalizes for the aerosol component in the atmosphere. In fact, Eq. (3) can also be approximated as [16]

$$T_{ind}(748,1240) \approx 1 + \frac{t(748)\rho_w(748)}{\rho_A(748)}, \tag{4}$$

where $t(748)\rho_w(748)$ and $\rho_A(748)$ are the TOA water-leaving reflectance [3] and aerosol reflectance (including Rayleigh-aerosol interactions) [3,21,22] at the wavelength 748 nm, respectively. Note that polarization effects are also included for both the Rayleigh $\rho_r(\lambda_l)$ and aerosol $\rho_A(\lambda_l)$ lookup tables [16,17,21]. Therefore, for the turbid waters, $T_{ind}$(748,1240) > 1 due to a non-zero ocean contribution at the band 748 nm, whereas for the open oceans $T_{ind}$(748,1240) ~1 because of the black ocean at the NIR bands (i.e., $\rho_w(748)$ ~0).

### *2.2. A Procedure for the NIR-SWIR Combined Atmospheric Correction*

The turbid water index $T_{ind}$(748,1240) can be used to discriminate productive and/or turbid ocean waters where there are non-zero NIR ocean contributions. Thus, with the detection of the turbid waters the SWIR atmospheric correction can be used for deriving ocean color products [12], and has shown significant improvements in MODIS ocean color products for cases with extremely turbid ocean waters [13].

*Shi and Wang* (2007) [16] used a threshold of $T_{ind}$(748,1240) >1.1 for the identification of the turbid waters using MODIS-Aqua measurements. The turbid water detection algorithm is quite effective and can be operated prior to the atmospheric correction procedure. However, we found from various tests that, to use the $T_{ind}$(748,1240) as a parameter for the algorithm switch between the NIR and SWIR methods, a threshold of 1.3 is the most appropriate choice due mainly to noise in $T_{ind}$(748,1240) when derived from SWIR bands. In addition, for cases with not too large NIR ocean contributions, the current modification [11] in accounting for the NIR ocean contributions usually works well. A study from cases along the U.S. east coast region (section 3.1) shows that, for cases with 1.1 < $T_{ind}$(748,1240) < 1.3, mean chlorophyll-a difference is usually within 5% between using the NIR and SWIR methods, while the mean difference is > 25% for cases of $T_{ind}$(748,1240) ≥ 1.3. Similar results are also obtained for the normalized water-leaving radiance at 443 nm. Due to considerably lower SNR values for the MODIS SWIR bands, it is generally better to use the NIR atmospheric correction algorithm for deriving MODIS ocean color products if it is applicable. Therefore, an approach using the $T_{ind}$(748,1240) parameter for the NIR-SWIR combined atmospheric correction procedure for MODIS ocean color data processing is proposed and summarized schematically as in Fig. 1:

#87508 - $15.00 USD Received 14 Sep 2007; revised 6 Nov 2007; accepted 6 Nov 2007; published 12 Nov 2007

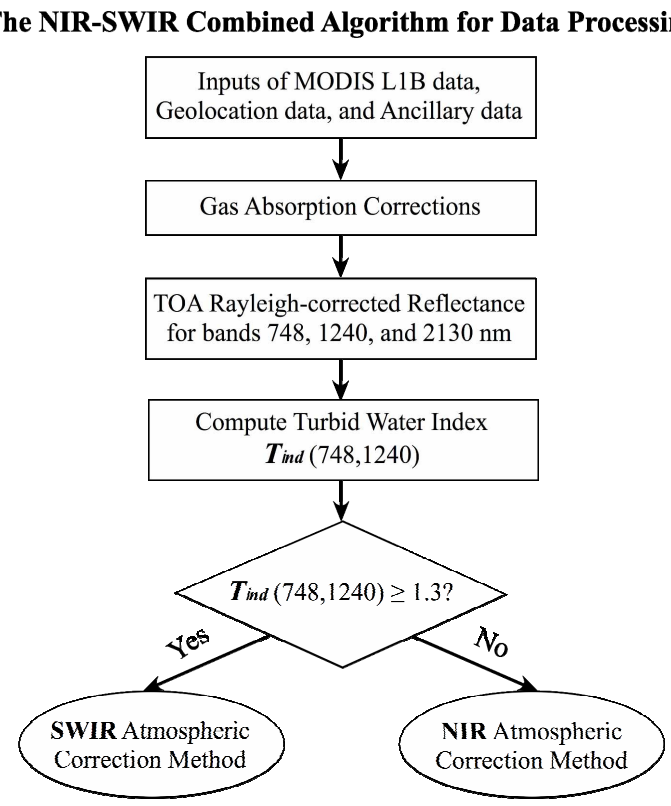


Fig. 1. The flow chart for the NIR-SWIR combined MODIS ocean color data processing procedure.

(1) With inputs of the MODIS L1B data, the corresponding MODIS geo-location data, and the ancillary data, the gas absorptions (e.g., water vapor) are corrected for the MODIS-measured TOA reflectances. This produces the MODIS $\rho_t(\lambda_l)$ values.

(2) From $\rho_t(\lambda_l)$ and the Rayleigh lookup tables, the Rayleigh-corrected reflectance $\Delta\rho^{(RC)}(\lambda_l)$ for MODIS bands 748, 1240, and 2130 nm are computed. The turbid water index $T_{ind}$(748,1240) can then be calculated using Eq. (3).

(3) For pixels with $T_{ind}$(748,1240) ≥1.3, the SWIR atmospheric correction algorithm is applied, while for cases with $T_{ind}$(748,1240) <1.3 the standard (NIR) atmospheric correction procedure is then executed for deriving MODIS ocean color products.

It is noted that, in the NIR-SWIR procedure, one may easily change the $T_{ind}$(748,1240) threshold for some specific regional data processing and applications.

### 3. Algorithm Performance Evaluation using MODIS Data

The proposed NIR-SWIR combined atmospheric correction approach has been implemented in the MODIS ocean color data processing and tested extensively using MODIS-Aqua measurements in various coastal regions. Here, we provide two examples from MODIS-Aqua measurements along the U.S. and China east coast regions for algorithm performance evaluation and assessment.

*3.1. Example Cases along the U.S. East Coast Region*

#87508 - $15.00 USD Received 14 Sep 2007; revised 6 Nov 2007; accepted 6 Nov 2007; published 12 Nov 2007

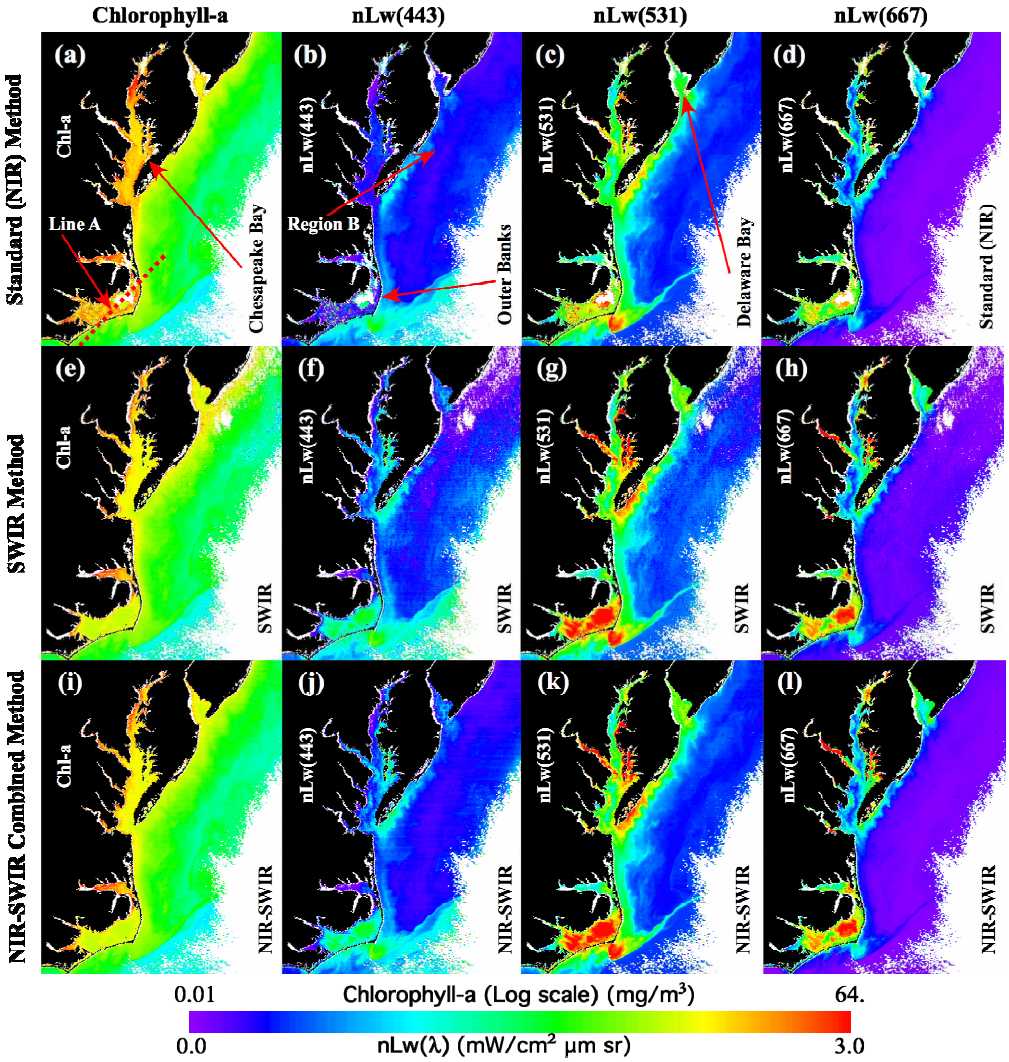


Fig. 2. The MODIS-Aqua measurements acquired along the U.S. east coast region on April 5, 2004 for the images of Chl-a, *nLw*(443), *nLw*(531), and *nLw*(667), respectively. Panels (a)-(d) are results from the standard (NIR) method; panels (e)-(h) are results from the SWIR method; and panels (i)-(l) are results from the NIR-SWIR combined method.

Figure 2 provides an example of algorithm performance comparisons using three different approaches along the U.S. east coast region that were observed by the MODIS Aqua on April 5, 2004. Results in the top panel of Fig. 2 (2(a)-2(d)) are MODIS-derived chlorophyll-a (Chl-a) concentration [24] and the normalized water-leaving radiances $nLw(\lambda)$ [3,4,25-27] at wavelengths 443 nm ($nLw(443)$), 531 nm ($nLw(531)$), and 667 nm ($nLw(667)$), respectively, which were obtained using the standard (NIR) data processing approach. Figures 2(e)-2(h) (the middle panel) are results corresponding to the same parameters derived using the SWIR atmospheric correction method, while images in Figs. 2(i)-2(l) (the bottom panel) are the corresponding results from using the NIR-SWIR combined data processing approach. The Chl-a concentration is scaled logarithmically from 0.01 to 64 ($mg/m^3$) and the values of $nLw(\lambda)$ for bands 443, 531, and 667 nm are all scaled linearly from 0–3 ($mW\ cm^{-2}\ \mu m^{-1}\ sr^{-1}$). Note that the line across the Outer Banks indicated as "Line A" in Fig. 2(a) is used later for a quantitative study for the algorithm performance (section 3.3). Data from "Region B" along

#87508 - $15.00 USD Received 14 Sep 2007; revised 6 Nov 2007; accepted 6 Nov 2007; published 12 Nov 2007

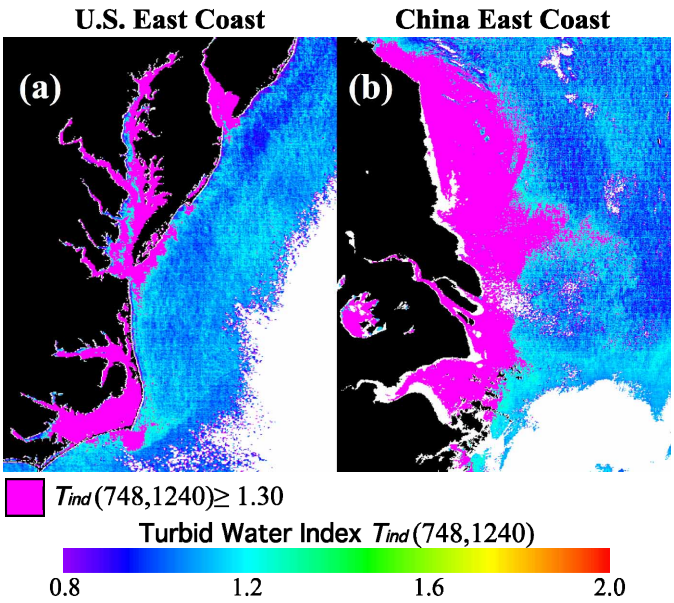


Fig. 3. The turbid water index $T_{ind}(748,1240)$ images corresponding to the MODIS results discussed for cases (a) along the U.S. east coast region (Fig. 2) and (b) along the China east coast region (Fig. 5). Pixels with the $T_{ind}(748,1240) \geq 1.3$ are masked in pink.

the coast in Fig. 2(b) are used for the data noise evaluation (later in this section). As discussed in the previous section, for deriving the ocean color results using the NIR-SWIR combined approach (Figs. 2(i)-2(l)), values of the turbid water index $T_{ind}(748,1240)$ were first computed for each pixel prior to the atmospheric correction. The MODIS-derived $T_{ind}(748,1240)$ image for this case (U.S. east coastal region) is shown in Fig. 3(a), where pixels with $T_{ind}(748,1240) \geq 1.3$ are masked in pink. The $T_{ind}(748,1240)$ value in Fig. 3 is scaled from 0.8-2.0. Thus, for the NIR-SWIR combined data processing (results in Figs. 2(i)-2(l)), the SWIR atmospheric correction is operated for the regions that are masked in pink in Fig. 3(a), while the standard (NIR) method is applied for all the other ocean regions.

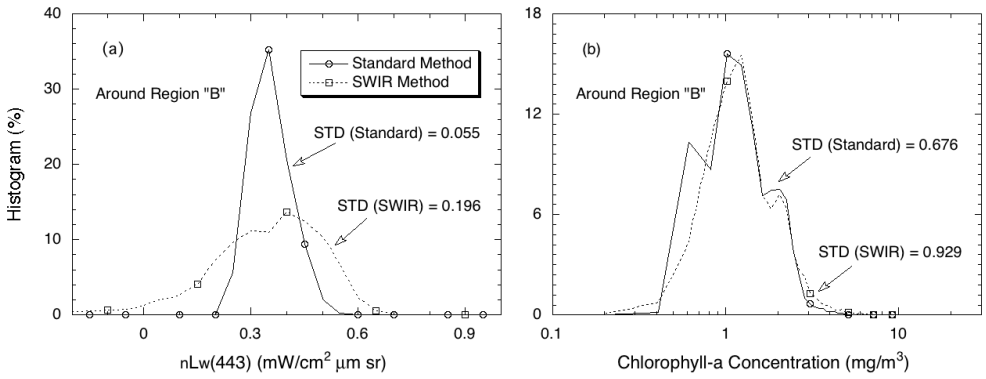


Fig. 4. Comparisons in histogram from the selected "Region B" indicated in Fig. 2(b) for the data noise evaluation for the MODIS-derived ocean color product of (a) $nLw(443)$ and (b) Chl-a.

Judging the results by examining overall image quality (e.g., data smoothness, number of missing data, etc.), Fig. 2 shows that, while the standard (NIR) method produces good quality ocean color products further offshore, the standard data processing outputs results with

#87508 - $15.00 USD Received 14 Sep 2007; revised 6 Nov 2007; accepted 6 Nov 2007; published 12 Nov 2007

noticeable noise and significant missing data in the coastal regions, e.g., regions in and/or around Chesapeake Bay, Outer Banks, and Delaware Bay. Alternatively, results in Figs. 2(e)-2(h) show that the SWIR algorithm can significantly improve the ocean color products in the coastal near-shore regions, but further offshore there is substantial noise and data dropout in the derived products, e.g., results from regions around the northern Delaware Bay. Thus, the advantages of using the NIR-SWIR combined method for the MODIS ocean color data processing are readily demonstrated in Figs. 2(i)-2(l). The new method has not only produced improved ocean color products in near-shore coastal regions, it also has preserved the high quality data products in further offshore.

Figure 4 provides examples of the data noise evaluation for the SWIR-derived products along the U.S. east coastal region (noted "Region B" in Fig. 2(b)). These are comparison results in histogram that are derived using the standard (NIR) and SWIR methods for products of $nLw(443)$ (Fig. 4(a)) and Chl-a (Fig. 4(b)). These results show a considerably increased standard deviation (STD) (i.e., noise) in the MODIS SWIR-derived $nLw(443)$ compared with that from the standard (NIR) method (Fig. 4(a)). In particular, for cases with low $nLw(\lambda)$ values (e.g., $nLw(443)$ in Fig. 4(a)), the SWIR method often produces more $nLw(\lambda) < 0$ cases than results from the standard (NIR) method. However, Fig. 4(b) shows a slightly increased STD value in the MODIS SWIR-derived Chl-a product. In this case, the noise level in the MODIS-derived Chl-a product is really comparable for both the standard (NIR) and SWIR methods.

### *3.2. Example Cases along the China East Coast Region*

The China east coastal region contains some of the most consistently highly turbid waters found in the global ocean. Figure 5 provides results of another example for the NIR-SWIR combined algorithm evaluation. The images are derived from the MODIS-Aqua measurements on October 19, 2003 along the China east coastal region. Figures 5(a)-5(d) are results obtained using the standard (NIR) method for the Chl-a and $nLw(\lambda)$ at wavelengths 443 nm ($nLw(443)$), 531 nm ($nLw(531)$), and 551 nm ($nLw(551)$), respectively. Figures 5(e)-5(h) are the same corresponding results derived using the SWIR method and Figs. 5(i)-5(l) are results from using the NIR-SWIR combined approach. In this case, we have shown results of $nLw(\lambda)$ at 551 nm instead of at 667 nm (Fig. 2) because of the problem with sensor saturation at band 667 nm in the various regions (e.g., the Hangzhou Bay). It is also noted that, compared to results in Fig. 2, the value of $nLw(\lambda)$ increases substantially and the upper-limit in images is now doubled, which is scaled from 0 to 6 (mW $cm^{-2}$ $\mu m^{-1}$ $sr^{-1}$). Similar to the case presented in Figs. 2 and Fig. 3(a), Fig. 3(b) shows the corresponding $T_{ind}(748,1240)$ results that are used for producing Figs. 5(i)-5(l) using the NIR-SWIR combined algorithm. In Figs. 5(i)-5(l), pixels with $T_{ind}(748,1240) \geq 1.3$ (masked in pink in Fig. 3(b)) are processed using the SWIR algorithm, while all others (with $T_{ind}(748,1240) < 1.3$) are processed using the standard (NIR) atmospheric correction algorithm.

Along the China east coast, the ocean is typically sediment-dominated [28] for which the MODIS-measured $nLw(\lambda)$ values increase as a function of wavelength from the blue to the green band, and $nLw(\lambda)$ values for some regions (e.g., the Hangzhou Bay) actually peak at the red band [13]. For such extremely turbid waters along the China east coast, the SWIR method has produced reasonable ocean color products (Figs. 5(e)-5(h)) compared with results from the standard (NIR) method (Figs. 5(a)-5(d)), in particular, data from regions in the Hangzhou Bay, Yangtze River Estuary, as well as inland Tai Lake. In these regions, the standard (NIR) method fails entirely. Further offshore, however, we can clearly see considerable noise and data dropout associated with products derived from the SWIR method (Figs. 5(e)-5(h)). Thus, the NIR-SWIR combined algorithm has again produced good quality data in both offshore and inshore (Figs. 5(i)-5(l)).

#87508 - $15.00 USD Received 14 Sep 2007; revised 6 Nov 2007; accepted 6 Nov 2007; published 12 Nov 2007

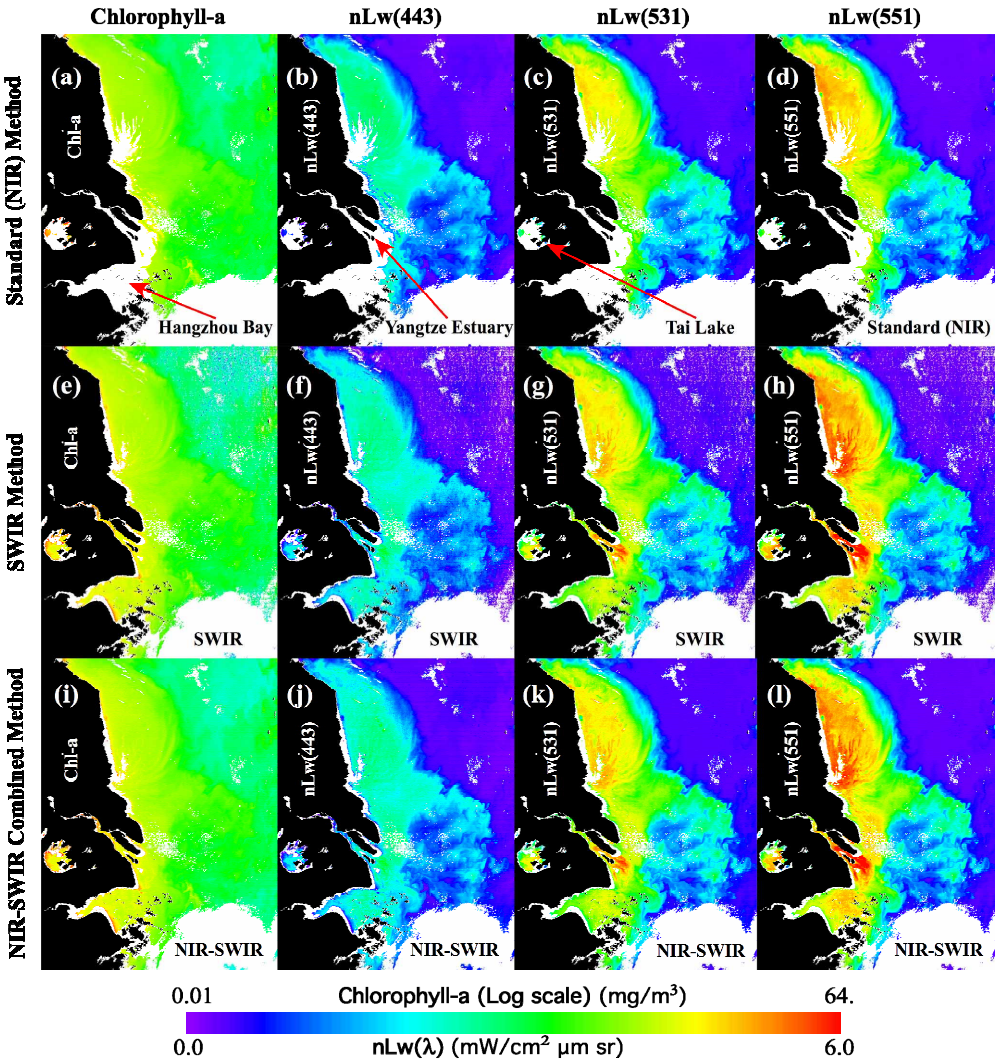


Fig. 5. The MODIS-Aqua measurements acquired along the China east coast region on October 19, 2003 for the images of Chl-a, *nLw*(443), *nLw*(531), and *nLw*(551), respectively. Panels (a)-(d) are results from the standard (NIR) method; panels (e)-(h) are results from the SWIR method; and panels (i)-(l) are results from the NIR-SWIR combined method.

### *3.3. Quantitative Evaluations*

We have studied the performance of the NIR-SWIR combined algorithm quantitatively, in particular, the product continuity between using the NIR method and SWIR approach. Figure 6 provides examples of these evaluations, focusing particularly on the data continuity with the algorithm switch between the NIR and SWIR methods. Figure 6 shows the MODIS-derived results as a function of the latitude in the line plot selected from the case along the U.S. east coast region, which is indicated as "Line A" in Fig. 2(a) (across the Outer Banks). Figures 6(a)-6(c) are the retrieved normalized water-leaving radiance $nLw(\lambda)$ at 443, 551, and 667 nm across the line using the standard (NIR) method, the SWIR method, and the NIR-SWIR combined method, respectively, while Fig. 6(d) compares results of the chlorophyll-a concentration using all three methods. In Fig. 6(d), values of the turbid water index $T_{ind}(748,1240)$ that were used to make switch between the NIR and SWIR methods for the NIR-SWIR combined algorithm are also provided (scale indicated in the bottom right side).

#87508 - $15.00 USD Received 14 Sep 2007; revised 6 Nov 2007; accepted 6 Nov 2007; published 12 Nov 2007

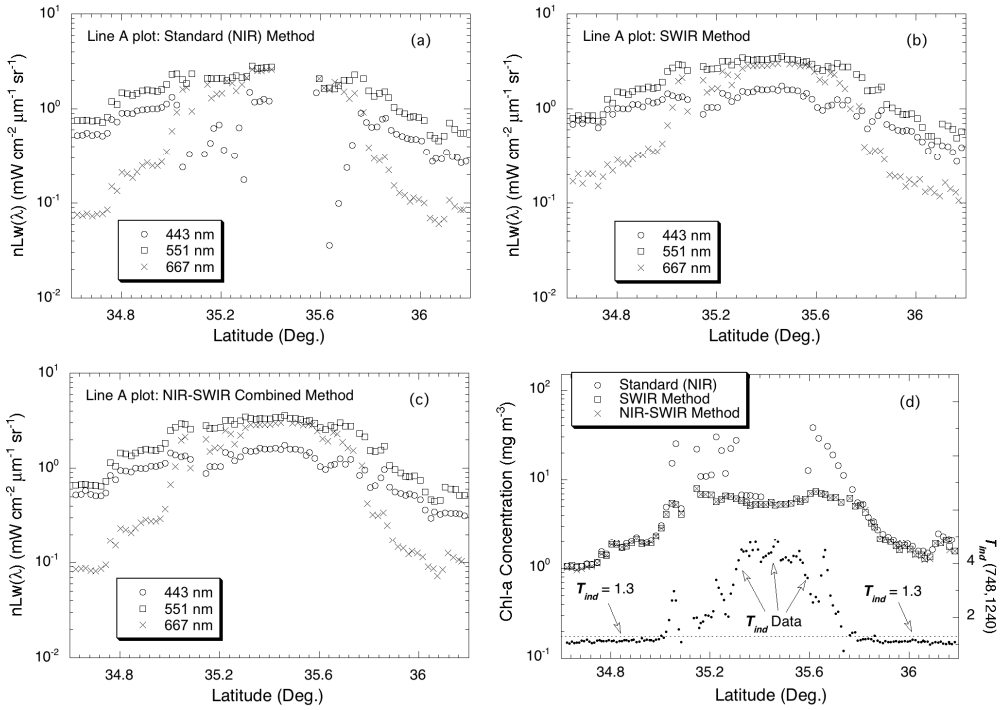


Fig. 6. The MODIS-derived $nLw(\lambda)$ at 443, 551, and 667 nm as a function of the latitude for the "Line A" shown in Fig. 2(a) using (a) the standard (NIR) method, (b) the SWIR method, and (c) the NIR-SWIR combined method. Plot (d) compares results of chlorophyll-a concentrations using the all three methods and values of the turbid water index $T_{ind}(748,1240)$ are also provided along the line (scale indicated in the bottom right side).

A dashed line with $T_{ind}(748,1240) = 1.3$ is plotted in Fig. 6(d), showing corresponding regions where products are derived either using the NIR method ($T_{ind}(748,1240) < 1.3$) or with the SWIR method ($T_{ind}(748,1240) \geq 1.3$) for the NIR-SWIR combined approach.

Results in Fig. 6(a) show that with the NIR method the MODIS-derived $nLw(\lambda)$ values have large errors in the latitudes ranging between 35.0° and 35.76° for which the $T_{ind}(748,1240) \geq 1.3$ (Fig. 6(d)). The $nLw(\lambda)$ values around the middle point of the line in Fig. 6(a) are either missing or with significant errors (biased low) due to the very turbid water in the Outer Banks. Using the SWIR method for the Outer Banks region, the retrieved $nLw(\lambda)$ values are much improved (Fig. 6(b)). However, for cases with $T_{ind}(748,1240) < 1.3$ (Fig. 6(d)), results derived from the SWIR method in Fig. 6(b) show slight differences as from the NIR method in Fig. 6(a). Figure 6(c) presents the results from the NIR-SWIR combined method, showing the same data quality offshore with improved products in the near-shore turbid waters. There are no obvious data discontinuities between using the NIR and SWIR methods. Furthermore, Fig. 6(d) has demonstrated the differences in the MODIS-derived chlorophyll-a values using the three approaches. The NIR-SWIR combined method produces continuous values for the chlorophyll-a product across the non-turbid and turbid waters. In addition, compared with the results from the NIR method, the chlorophyll-a values are substantially reduced using the SWIR algorithm in the Outer Banks (i.e., inshore waters).

Figure 7 provides quantitative comparisons in histogram using the three different algorithms for the MODIS-derived ocean color products in the Outer Banks region (around "Line A" in Fig. 2(a)). Figures 7(a)-7(c) show histogram results for the MODIS-derived $nLw(\lambda)$ at 443, 531, and 667 nm, respectively, while Fig. 7(d) is results of the MODIS Chl-a product. Each plot in Fig. 7 has three curves corresponding to the MODIS data processed

#87508 - $15.00 USD Received 14 Sep 2007; revised 6 Nov 2007; accepted 6 Nov 2007; published 12 Nov 2007

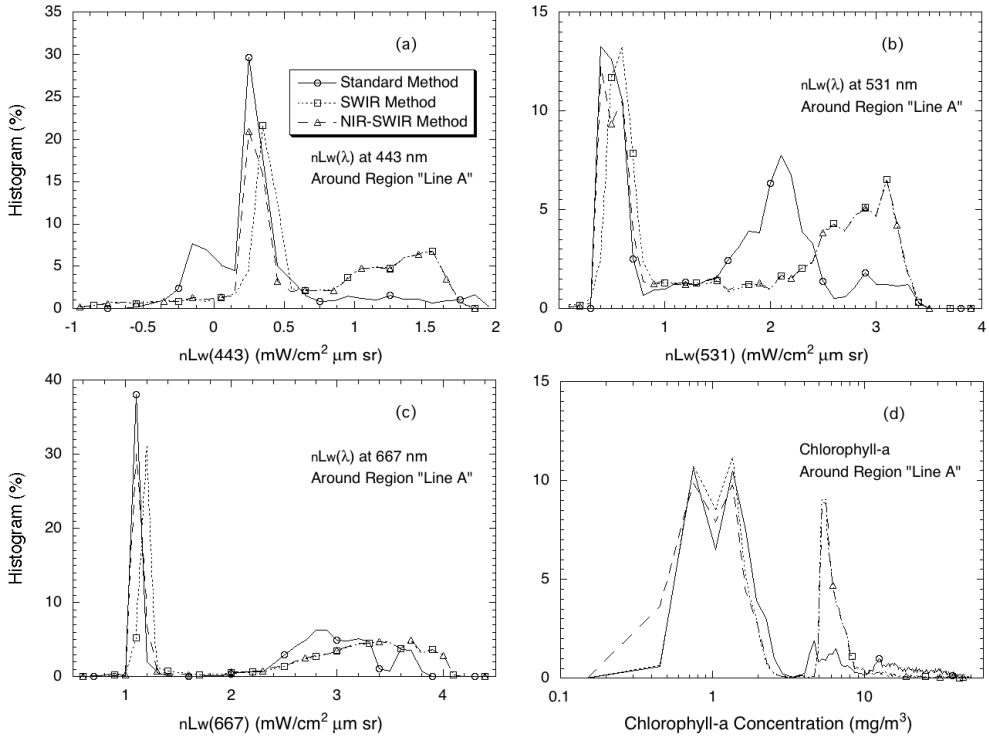


Fig. 7. Comparisons in histogram using the three different algorithms for the MODIS-derived ocean color products from the region around "Line A" in Fig. 2(a) for (a) *nLw*(443), (b) *nLw*(531), (c) *nLw*(667), and (d) Chl-a.

using the standard (NIR), SWIR, and NIR-SWIR combined method. Results in Fig. 7 demonstrate that, for the *nLw*(λ) product, the standard (NIR) and SWIR methods produce values consistently (but with some slight differences) at the non-turbid waters (lower value peaks), whereas for the turbid waters (in the Outer Banks) there are significant differences in the derived *nLw*(λ). It is noted that, however, for the *nLw*(443) data in Fig. 7(a) the standard (NIR) algorithm produced a peak in histogram with *nLw*(443) <0. For the Chl-a comparison, results are again consistent for the non-turbid ocean waters with histogram peaked at ~1 (mg/m$^3$), but there are considerable differences in the MODIS-derived Chl-a values for the turbid waters (in the Outer Banks). For the Outer Banks region, the SWIR method has a Chl-a peak at ~5-6 (mg/m$^3$), while the standard (NIR) method produced large Chl-a values extended up to ~20-30 (mg/m$^3$). Thus, results in Fig. 7 demonstrated that the NIR-SWIR combined approach has produced the MODIS ocean color products consistently with the standard (NIR) and SWIR methods in the non-turbid and turbid waters, respectively.

## 4. Conclusions

We have presented in here an approach for MODIS ocean color data processing using combined NIR and SWIR bands for atmospheric correction. In general, for the global open oceans and offshore waters, MODIS-Aqua has been producing good quality ocean color products using the standard (NIR) atmospheric correction algorithm. However, for the coastal waters, further improvements in the products are required, due to the occurrence of very turbid waters for which the ocean is non-black at the NIR bands. For turbid waters, the MODIS SWIR bands can be used for atmospheric correction [10,12,20]. Indeed, the SWIR algorithm has been developed and demonstrated to produce reasonable ocean color products in the China east coast where waters are consistently extremely turbid [13]. On the other

#87508 - $15.00 USD Received 14 Sep 2007; revised 6 Nov 2007; accepted 6 Nov 2007; published 12 Nov 2007

hand, because of substantially lower sensor SNR values for the MODIS SWIR bands, it is required that the SWIR algorithm be applied only to turbid water cases (pixels), whereas for the open oceans/offshore waters the data are still processed using the NIR algorithm. Using the turbid water index $T_{ind}(748,1240)$ [16] as the indicator for productive and turbid ocean regions, we have developed an approach using the NIR-SWIR combined atmospheric correction algorithm for MODIS ocean color data processing.

The performance of the NIR-SWIR combined approach has been tested and evaluated and two examples from MODIS measurements acquired along the U.S. and the China east coast regions are provided. Results show that using the NIR-SWIR combined method the MODIS-derived ocean color products have been improved in near-shore turbid waters, while at the same time high quality products in offshore waters have been preserved. We have particularly looked into the data continuity issue using the new approach, demonstrating that there are no obvious discontinuities in the derived products between using the NIR and SWIR methods. The data products from the NIR-SWIR combined method appear to be very reasonable. Therefore, the new approach in the data processing can be used for continuously and simultaneously producing good quality MODIS ocean color products in offshore waters and in the global open oceans, as well as improved data along near-shore coastal regions.

**Acknowledgments**

This research was supported by the NASA EOS MODIS grant. We thank two anonymous reviewers for their helpful comments. The views, opinions, and findings contained in this paper are those of the authors and should not be construed as an official NOAA or U.S. Government position, policy, or decision.

#87508 - $15.00 USD Received 14 Sep 2007; revised 6 Nov 2007; accepted 6 Nov 2007; published 12 Nov 2007